Received 30 March 2021
Revised 27 May 2021
Accepted 9 June 2021

Flow control in microfluidics devices: electro-osmotic Couette flow with joule heating effect

C. Ahamed Saleel and Saad Ayed Alshahrani
Mechanical Engineering Department, College of Engineering, King Khalid University, Abha, Saudi Arabia
Asif Afzal
Mechanical Engineering, PA College of Engineering, Mangalore, India
Maughal Ahmed Ali Baig
Mechanical Engineering, CMR Technical Campus, Secunderabad, India, and
Sarfaraz Kamangar and T.M. Yunus Khan
Mechanical Engineering Department, College of Engineering, King Khalid University, Abha, Saudi Arabia

Abstract

Purpose – Joule heating effect is a pervasive phenomenon in electro-osmotic flow because of the applied electric field and fluid electrical resistivity across the microchannels. Its effect in electro-osmotic flow field is an important mechanism to control the flow inside the microchannels and it includes numerous applications.

Design/methodology/approach – This research article details the numerical investigation on alterations in the profile of stream wise velocity of simple Couette-electroosmotic flow and pressure driven electro-osmotic Couette flow by the dynamic viscosity variations happened due to the Joule heating effect throughout the dielectric fluid usually observed in various microfluidic devices.

Findings – The advantages of the Joule heating effect are not only to control the velocity in microchannels but also to act as an active method to enhance the mixing efficiency. The results of numerical investigations reveal that the thermal field due to Joule heating effect causes considerable variation of dynamic viscosity across the microchannel to initiate a shear flow when EDL (Electrical Double Layer) thickness is increased and is being varied across the channel.

Originality/value – This research work suggest how joule heating can be used as en effective mechanism for flow control in microfluidic devices.

Keywords Couette flow, Electro-osmotic flow, Zeta potential, Joule heating effect, Microchannels, Electrical double layer, Mixing in microchannels, Flow control

Paper type Research paper

Nomenclature

C_p	Specific heat at constant pressure	E	Strength of the externally-applied electric field
D	Dielectric constant		

Frontiers in Engineering and Built Environment
Vol. 1 No. 2, 2021
pp. 146-160
Emerald Publishing Limited
e-ISSN: 2634-2502
p-ISSN: 2634-2499
DOI 10.1108/FEBE-03-2021-0020

The authors extend their appreciation to the Deanship of Scientific Research at King Khalid University for funding this work through the research groups program under grant number R.G.P.2/74/41.

Conflicts of interest: The authors declare that there is no conflict of interests regarding the publication of this paper

H	Channel Height	β	Non-dimensional parameter relating α, ω and H
T	Temperature		
U	velocity at the outer edge of EDL	γ	The factor representing the change of viscosity in the flow field with respect to temperature
$\overrightarrow{V}$	Velocity vector		
EDL	Electrical Double Layer		
FVM	Finite volume method	λ	Debye length or EDL thickness
PSOR	Point Successive Over Relaxation	μ	Dynamic viscosity
TDMA	Tri-diagonal matrix algorithm	ε	Permittivity of fluid
e	Electron charge	ρ	Fluid density
k_b	Boltzmann constant	ψ	Electro-osmotic potential
n_0	Bulk flow ion density	ζ	zeta potential
p	Pressure	φ	External electric potential
t	Time	ρ_e	Charge density
z	Valence of the electrolyte/fluid	ω	Debye-Huckel parameter (reciprocal of EDL thickness, λ)
α	The ionic energy parameter		

1. Introduction

1.1 Electro-osmotic flow

The chemical state of the dielectric solution present in most of the microfluidic devices changes due to the presence of charged surfaces of the microchannel walls. The EDL consists of a stationary inner layer and an outer diffuse layer (Probstein, 2005). Oppositely charged ions in solution is attracted towards these charged surfaces in the EDL. A flow can be initiated with the help of an externally applied electric field (Masliyah, 2021) and is tangential to the microchannel wall surfaces due to the presence of viscous drag. The type of flow is termed as "Electro-osmotic flow (EOF) or Electro-osmosis" was originally referred in the year 1809 by F.F. Reuss in his research manuscript published in the Proceedings *of the Imperial Society of Naturalists of Moscow* (Reuss, 1809). Figure 1 illustrates the electro-osmotic flow. The research related to the flow and the related transport mechanisms in microfluidics are getting wide popularity among the researchers and numerous applications of the same have been cited in recent review articles. Among different mechanisms to control flow in microfluidic gadgets, the electro-osmotic effects are being developed as a promising method, especially under the profoundly viscous situations for highly laminar flow regimes in which the Reynolds number is less than the unity.

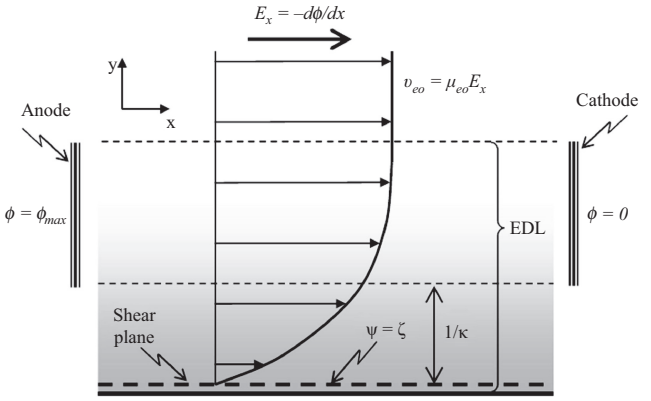

Figure 1.
Electro-osmotic flow

Apart from electro-osmosis, the other electro-kinetic phenomena are (1) Electrophoresis, (2) Streaming potential, and (3) Sedimentation potential. Right from its explanation by F.F. Reuss, EOF has been employed for various applications: drying soil in civil engineering/soil mechanics related applications, elimination of contaminants in the soil in land reclamation projects (Probstein and Hicks, 1993) or in the desalination of salt water (Probstein, 1972). Due to the significance of its modern applications in micro-fluidics, those early applications have now been entirely phased out. EOF is the principal electro-kinetic phenomenon utilized in micro-fluidic devices. This phenomenon can be efficiently used for fluid control and handling by suitable application of electric fields. EOF control eliminates most of the moving mechanical components thus mechanical failures due to fatigue and fabrication defects are totally ruled out. Electro-osmotic pumps are widely used for drug delivery and biomedical pumping applications.

Since the introduction of electro-kinetic effects by Reuss in 1809 (Reuss, 1809) many scientists have been conducting researches in the field of microfluidics. The EDL theory was proposed by Helmholtz in 1870 and it correlates the flow and the electrical parameters for electrokinetically enabled transport phenomena.

Solution of combined pressure driven/electro-osmotic flows in two-dimensional slits or microchannels (Ohshima, 1990; Dutta and Beskok, 2001a, b), as well as in thin cylindrical capillaries (Rice, 1966; Lo and Chan, 1994) constitute the major theoretical developments. Irrotationality of interior electro-osmotic flows for randomly shaped geometries are proposed by Santiago (2001). Cummins *et al.* (2000) identified the ideal electroosmosis concept (i.e. EOF in the absence of external pressure gradient) and showed the similarity between the velocity and electric fields under specific outer field boundary conditions. Recent research works in the field of electroosmotic flow are proposed by Santiago (2001) and Dutta and Beskok (2001a, b).

1.2 Joule heating effect and its use in flow control

Pure EOF velocity is having a plug-shaped profile (Paul *et al.*, 1998; Nithiarasu, 2005) with little hydrodynamic dispersion which is needed for sample delivery and detection in microfluidic devices. In practice, however, according to Rozing (2018), alterations to the plug shape happens because of many reasons such as sample overloading, longitudinal diffusion, adsorption of species on micro-channel walls, electric field and non-uniform zeta potential, non-uniform geometry, and Joule heating effect. This research article is all about the Joule heating effect and how it affects EOF velocity profiles in micro-fluidic devices/systems. Joule heating effect is named after James Prescott Joule, who proposed this effect.

Joule heating effect is a pervasive phenomenon in electro-osmotic flow due to the applied electric field across the microchannels. Its effect in electro-osmotic flow field is an important mechanism to control the flow inside the microchannels and its applications include separation techniques by means of electro kinetic effects such as electrochromatography, transportation and manipulation of dielectric fluids, molecules and cells, various chemical and biological processes in lab-on-chip devices. Even though the Joule heating effect is desirable for efficient operating conditions of various microfluidic devices, effective dissipation of the heat generated is crucial for efficient electro kinetic systems. The disadvantages of Joule heating effect include an increase in the overall temperature inside the microchannels along the transverse and longitudinal directions may cause denaturation of proteins, DNA, and various biological samples. Therefore, Joule heating effect sets a maximum limit for the usage of high electrical voltages for many applications (Evenhuis, 2007; Rathore, 2004). The research work with regard to Joule heating effect has to be given due importance and its results are helpful for the optimal design and highly efficient microfluidic devices apart from this effect's exploitation as a flow control mechanism in microfluidic devices.

Three methods are usually used for flow control in microfluidic and nanofluidic devices: (1) hydrostatic pressure difference, (2) syringe pumps, and (3) liquid pumps. Electroosmotic pumps are the beat substitute for common liquid pumps in which joule heating effect may be wisely used for flow control by varying the applied external electric field across the microchannels. hydrostatic pressure difference is the easiest method for flow control in microfluidic systems. Syringe pumps are first artificial flow control method used in microfluidic and nanofluidic devices. Originally it was devised for perfusion systems in the field of medical science and were later employed by microfluidic scientific community in its initial developments. The major disadvantages include the progress of pulsatile flows at very low flow rates and more span of time to stabilize the effective rate of flow when non-uniform tubing is used in the microfluidic devices. The third type, i.e. liquid pumps cannot be modelled as suitable flow control device as the developed back pressure decelerates the flow rate in most of the microfluidic applications. Some liquid pumps used in microfluidic devices are peristaltic pumps and piezo-electric pumps. The peristaltic pumps permit the usage of interchangeable flexible tubes and are suitable for the devices with greater flow rates, whereas the piezo-electric pumps are compact in size and is suitable for medium flow rates. But, electro-osmotic pumps with the joule heating effect are far superior to aforementioned flow control techniques. Its advantages include the absence of the fluctuation problems due to the usage of electric field and support larger back pressures. The disadvantage includes the requirements of low conductivity liquids.

The EOF velocity proposed by Helmholtz-Smoluchowski is given in the following equation,

$$U = \frac{E\varepsilon\zeta}{\mu} \tag{1}$$

The induced electric potential at the shear plane is termed as the zeta potential, ζ. The regulation of zeta potential is an excellent idea for the flow control in microfluidic devices and was proposed by Schasfoort *et al.* (1999). Importance of Couette flow in microfluidics are cited in Ali *et al.* (2007), Kaurangini and Jha (2011), Izquierdo *et al.* (2015), Chen and Tian (2009).

It is understood that lots of difficulties are associated with the performance of experimentation in microfluidic/nanofluidic devices. Hence, it is always advised to develop steadfast numerical models and subsequent investigations in complex microfluidic geometries. Inter related effects of the pressure, viscous and inertial forces, and electroosmotic effects can be understood by the developed numerical models. Hence, the numerical results are helpful in design of optimal microfluidic devices before the actual fabrication and experimental verifications.

2. Governing equations

The Gou-Chapman model is used to study the electro-osmosis. This section provides the governing equations that form the basis of the theoretical modelling of Joule heating in electro-osmotic flow. The given equations administer the momentum (flow field), electricity (electric field) and transport of heat (temperature field) involved in electro-osmotic flow. They are

$$\nabla.\vec{V} = 0 \tag{2}$$

$$\rho\left[\frac{\partial\vec{V}}{\partial t} + \vec{V}.\nabla\vec{V}\right] = -\nabla p + \nabla.\left(\mu\nabla\vec{V}\right) + \rho_e\vec{E} \tag{3}$$

$$\rho C_p \left[\frac{\partial T}{\partial t} + \vec{V}.\nabla T\right] = \nabla.(k\nabla T) \tag{4}$$

The governing equations are deduced for electro-osmosis based on the standard approximations. In Eqn (3), the charge density, ρ_e follows the Boltzmann distribution:

$$\rho_e = -2zen_0 \sinh\left(\frac{ze\psi}{k_b T}\right) \tag{5}$$

The distribution of ions in the buffer solution is influenced by the static charge on the wall surface and is governed by the Poisson–Boltzmann equation:

$$\nabla^2(\psi) = -\frac{4\pi\rho_e}{D} \tag{6}$$

The externally imposed electric field is governed by

$$E = -\nabla\phi \tag{7}$$

Where the external electric potential, ϕ is governed by

$$\nabla.(\sigma\nabla\phi) = 0 \tag{8}$$

2.1 Temperature dependent physical properties

It is understood that the physical properties present in the governing Eqns (2)–(8) depend on temperature and the dynamic viscosity is the most sensitive to temperature. It can be assumed that the dynamic viscosity of dielectric solution is almost equal to that of pure water. The relation between the dynamic viscosity of dielectric solution and temperature is given as follows and is known to decrease with temperature (Saleel *et al.*, 2020).

$$\mu(T) = 2.761 \times 10^{-6} \exp\left[\frac{1713}{T}\right]\left(\frac{Ns}{m^2}\right) \tag{9}$$

Figure 2 shows the graphical form of Eqn (9) between zero and 100 degree Celsius. This describes that variation of dynamic viscosity with respect to temperature is significant and the profile is linear at usual temperature range wherein the micro-fluidic devices are operated. It is understood that Joule heating effect is a viable method for flow control in microfluidic devices.

To ease the study, the following assumptions are incorporated in the governing equations and are being enumerated as follows. The flow can be treated as two dimensional, laminar, and incompressible. The two-dimensional nature is justified because of the channel height is much smaller than the channel width. Body forces are negligible; hence the flow is assumed to be horizontal. All the walls follow no slip boundary conditions and the fluid follows Newton's law of viscosity. Since the plate and the walls of the channel are infinitely long, the stream lines are considered to be parallel and the flow is fully developed (i.e. $v = 0$), or $u = u(y)$. The electrical field strength applied across the flow direction in the micro-channels and is uniform and constant. Channel is experienced a constant vertical temperature difference, ΔT; the temperature boundary conditions are given as

$$T(x) = T_0 \quad \text{at } y = 0 \tag{10}$$

$$T(x) = T_0 + \Delta T \quad \text{at} \quad y = H \tag{11}$$

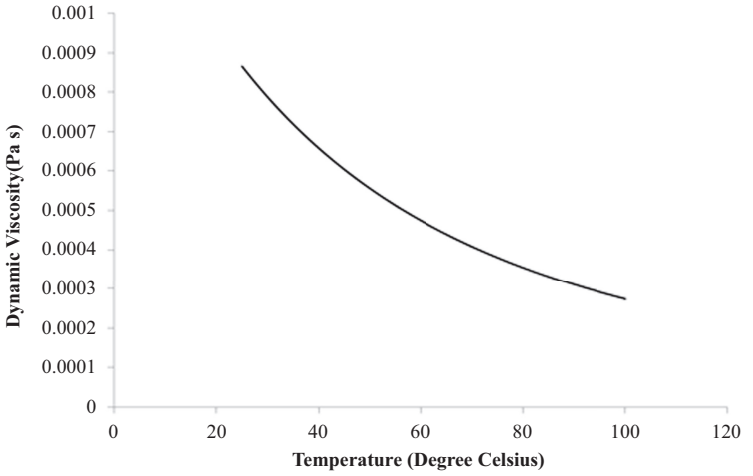

Figure 2.
Variation of dynamic viscosity with respect to temperature

$$\frac{d}{dy}\left(k\frac{dT}{dy}\right) = 0 \tag{12}$$

The solution of Eqn (12) with given boundary conditions is

$$\frac{T - T_0}{\Delta T} = \frac{y}{H} \tag{13}$$

Thus, the distribution of temperature is a linear function of y. The flow field governing equations are reduced to

$$\frac{\partial u}{\partial x} = 0 \tag{14}$$

$$-\frac{\partial p}{\partial x} + \frac{\mu}{\rho}\frac{\partial^2 u}{\partial y^2} + \frac{\rho_e}{\rho}E_x = 0 \tag{15}$$

$$\frac{1}{\rho}\frac{\partial p}{\partial y} = 0 \tag{16}$$

In order to establish a relation between the dynamic viscosity and temperature, a simple linear expression is assumed as shown below.

$$\mu = \mu_0\left[1 - \gamma\frac{T - T_0}{\Delta T}\right] = \mu_0\left[1 - \gamma\frac{y}{H}\right] \tag{17}$$

Substituting Eqn (17) in to Eqn (15), we have

$$-\frac{\partial p}{\partial x} + \frac{\partial}{\partial y}\left(\mu_0\left[1 - \gamma\frac{y}{H}\right]\frac{\partial u}{\partial y}\right) - \frac{DE_x}{4\pi}\frac{\partial^2 \psi}{\partial y^2} = 0 \tag{18}$$

2.2 Normalization

The spatial variables are normalized by the channel height, H; wall potential is normalized by zeta potential, ζ; pressure is normalized by viscous forces, $\frac{\mu_0 u_{\text{ref}}}{H}$; velocity is normalized by

Helmholtz-Smoluchowski velocity, $-\frac{E_x \epsilon \zeta}{\mu_0}$. Finally, Eqn (18) in non-dimensional form is expressed as follows:

$$\frac{\partial p^*}{\partial x^*} = \left(1 - \gamma \frac{y}{H}\right) \frac{\partial^2 u^*}{\partial y^{*2}} - \gamma \frac{\partial u^*}{\partial y^*} + \frac{\partial^2 \psi^*}{\partial y^{*2}} \tag{19}$$

The non-dimensional form of Eqn (6) is

$$\frac{\partial^2 \psi^*}{\partial y^{*2}} = \beta \sinh(\alpha \psi^*) \tag{20}$$

Here α is known as the ionic energy parameter which is termed as

$$\alpha = \frac{ze\zeta}{k_b T} \tag{21}$$

And β is the non-dimensional parameter relating α, ω and H.

$$\beta = \frac{(\omega H)^2}{\alpha} \tag{22}$$

where ω is the reciprocal of EDL thickness, which is given by

$$\omega = \frac{1}{\lambda} = \sqrt{\frac{8\pi z^2 e^2 n_0}{D k_b T}} \tag{23}$$

2.3 Physical significance of α *and* β

At 20°C, $\zeta = 25.4$ mV corresponds to $\alpha = 1$. When the value of ζ is doubled, the value of α is equals 2 and so on. If the channel height is 100 μm, the EDL thickness corresponding to different values of β is being depicted in Table 1.

It is obvious that the thickness of EDL is increased as the value of β is increased.

2.4 Solution methodology

FVM is used for the discretization of the prescribed governing equations with their suitable boundary conditions with the integration of the spatial-temporal of the conservation equations. Initially, Eqn (20) is being solved numerically and is quite challenging due to the exponential nonlinearity associated with the hyperbolic-sine function. In order to eliminate

Table 1. Significance of β

λ: EDL thickness (μm)	Debye-Huckel parameter $\omega = \frac{1}{\lambda}$	λ: EDL thickness (μm)	EDL thickness as a fraction of channel height	Ionic energy parameter, α	Channel height, H (μm)	$\beta = \frac{(\omega H)^2}{\alpha}$
1.0	10^6	1.0	1/100	1	100	10000.0
3.125	320×10^3	3.125	1/32	1	100	1000.0
10.0	10^5	10.0	1/10	1	100	100.0
31.6	31.65×10^3	31.6	1/3.2	1	100	1.0

these challenges, a Taylor series expansion of the right-hand side term is employed for linearization of the nonlinear source term of Eqn (20), and the equation is then solved by using point successive over-relaxation (PSOR) method, which is a variant of the Gauss–Seidel method for solving a linear system of equations that results in faster convergence. The numerically obtained electro-osmotic potential distribution is compared with the analytical solution of Eqn (20) by eliminating the nonlinearity with Debye-Huckel guesstimate which is effective only when $\zeta \leq 25.4$ mV (Saleel *et al.*, 2013; Saleel *et al.*, 2020). The numerically obtained electro-osmotic potential is impregnated in Eqn (19) and is being solved by powerful and accurate TDMA.

3. Results and discussions

The theoretical (analytical) and numerical solutions of the electro-osmotic potential distribution across the channel as a function of various values of β for a constant value of $\alpha = 1.0$ are depicted in Figure 3. As it is understood from Figure 3, thickness of EDL increase and covers the entire channel with the decrease in the value of β. When $\beta = 1.0$, there is disparity between analytical and numerical solutions. The reason for the same is explained as follows. The analytical solution is only valid with Debye-Huckel assumption and is invalid when the value of β decreases as well as when the value of α increases. For the high value of β, the EDL is confined and restricted to the channel walls, results in sharp variations in the distribution of electro-osmotic potential. It is obvious that for a constant value of β and for different increased values of α, the curves show an abrupt decay of the electro-osmotic. Figure 4 shows the theoretical (analytical) and numerical solutions of pure electroosmotic flow velocity across the channel as a function of various values of β at a constant value of $\alpha = 1.0$.

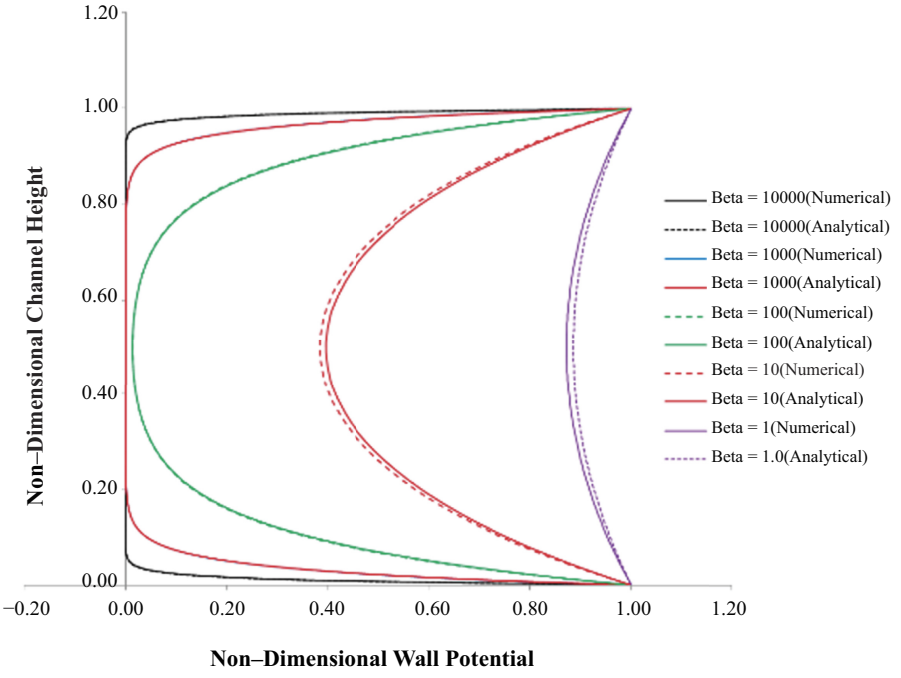

Figure 3.
Numerical and analytical variation of wall potential across the channel height for different values of β when $\alpha = 1$

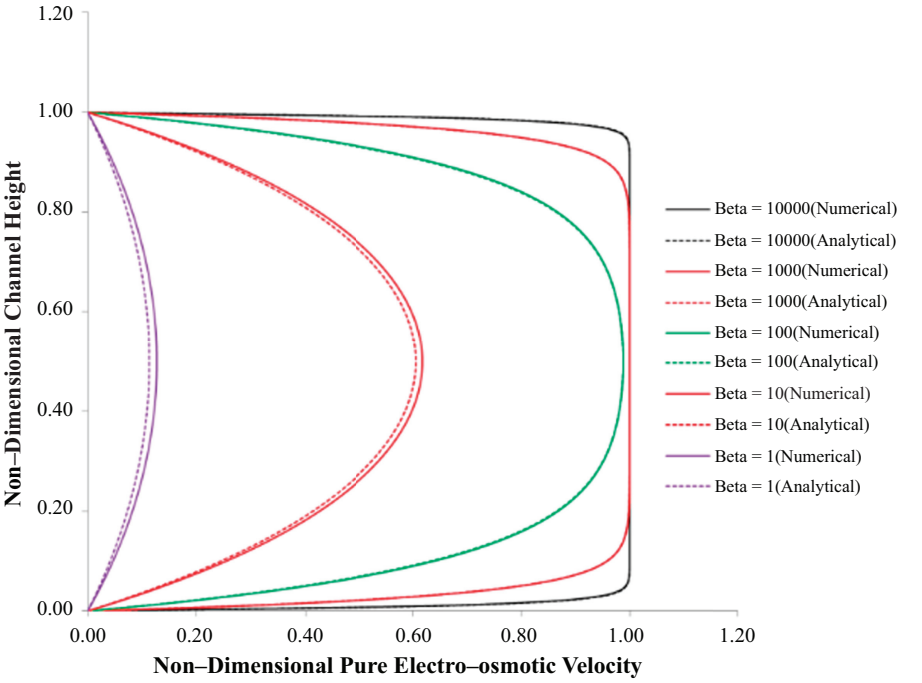

Figure 4.
Numerical and analytical variation of pure electro-osmotic velocity across the channel height for different values of β when $\alpha = 1$

It is clear that when the value of β is decreased, the profile deviates gradually from "plug shape" which is the characteristic feature of pure electro-osmotic flow with thin EDL.

Numerical solution of stream wise velocity electro-osmotic Cuette flow is depicted in Figure 5 when $\beta = 10000.0$, in Figure 6 when $\beta = 1000.0$, in Figure 7 when $\beta = 100.0$, in Figure 8 when $\beta = 10.0$ and in Figure 9 when $\beta = 1.0$. Here the velocity profile is plotted across

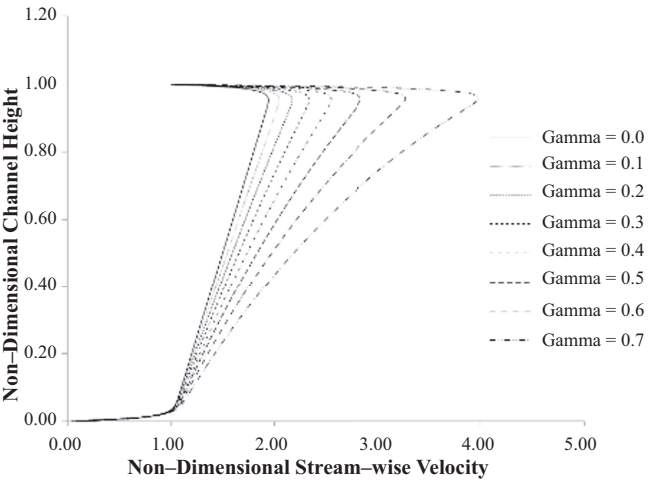

Figure 5.
Numerical variation of stream wise velocity in electro-osmotic Couette flow across the channel height with joule heating effect when $\beta = 10000$ and $\alpha = 1$

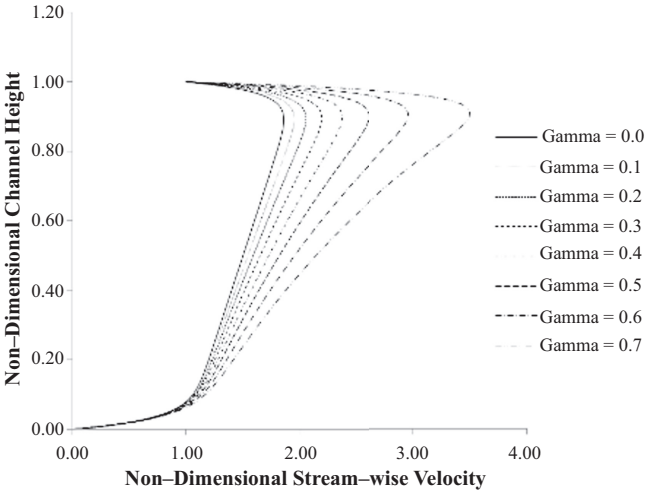

Figure 6.
Numerical variation of stream wise velocity in electro-osmotic Couette flow across the channel height with joule heating effect when $\beta = 1000$ and $\alpha = 1$

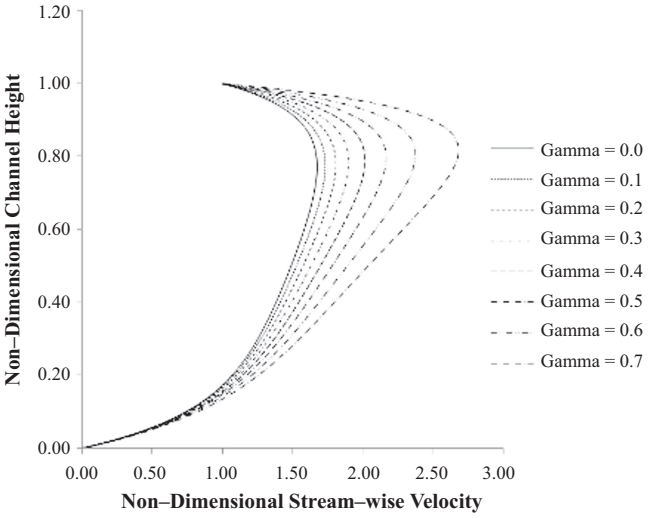

Figure 7.
Numerical variation of stream wise velocity in electro-osmotic Couette flow across the channel height with joule heating effect when $\beta = 100$ and $\alpha = 1$

the channel height with joule heating effect when $\alpha = 1.0$. As the value of Gamma increases from 0.1 to 0.7, it progressively accommodates the significance of temperature-dependent dynamic viscosity in flow silhouette. Gamma = 0.0 denotes the temperature independent dynamic. As Gamma increases, the viscosity of the dielectric fluid drops; this in sequence results in an elevation of velocity. As an outcome, the flow gradually starts tilting towards the upper plate as Gamma becomes larger and larger since the upper wall is hotter compared to the bottom wall.

Numerical solution of stream wise velocity in pressure driven electro-osmotic Couette flow is shown in Figure 10 when $\beta = 10000.0$, in Figure 11 when $\beta = 1000.0$, in

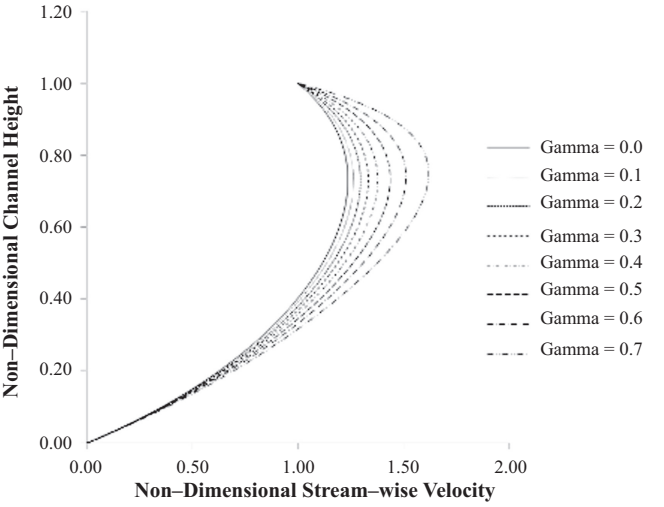

Figure 8.
Numerical variation of stream wise velocity in electro-osmotic Couette flow across the channel height with joule heating effect when $\beta = 10$ and $\alpha = 1$

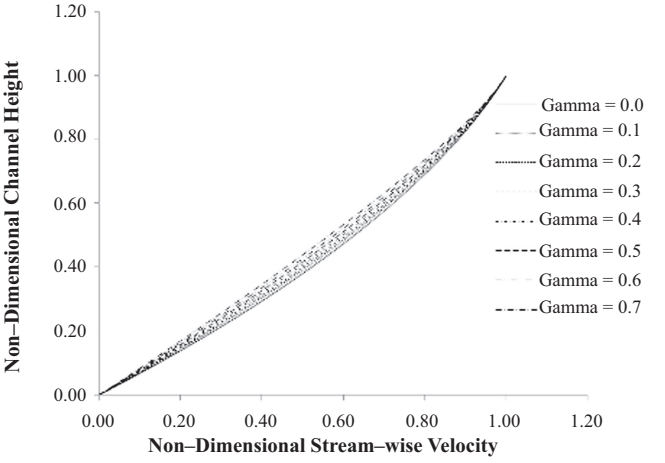

Figure 9.
Numerical variation of stream wise velocity in electro-osmotic Couette flow across the channel height with joule heating effect when $\beta = 1$ and $\alpha = 1$

Figure 12 when $\beta = 100.0$, in Figure 13 when $\beta = 10.0$ and in Figure 14 when $\beta = 1.0$. Here the velocity profile is plotted across the channel height with joule heating effect when $\alpha = 1.0$.

As the value of Gamma increases from 0.1 to 0.7, it progressively incorporates the significance of temperature-dependent dynamic viscosity in flow profile. Gamma = 0.0 denotes the temperature independent dynamic. As Gamma increases, the viscosity of the dielectric fluid drops; this in turn results in an elevation of velocity. As an outcome, the flow gradually starts tilting towards the upper plate as Gamma becomes larger and larger since the upper wall is hotter compared to the bottom wall.

The results of the current numerical simulations reveal that the flow control in microfluidic devices is possible with the increased non-uniform pure EOF-Couette/pressure driven Couette-EOF velocity field. The normal "plug-like" shape is deviated and this deviation may be helpful in flow control in electroosmotic pumps. The deviation from its

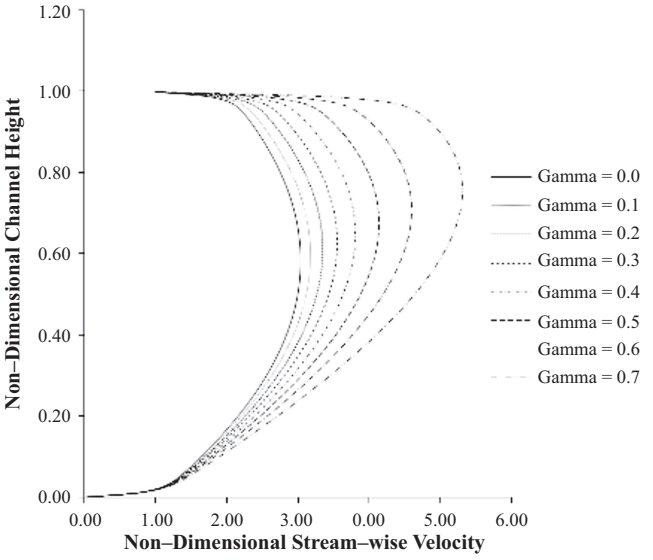

Figure 10.
Numerical variation of stream wise velocity in pressure driven electro-osmotic Couette flow across the channel height with joule heating effect when $\beta = 10000$ and $\alpha = 1$

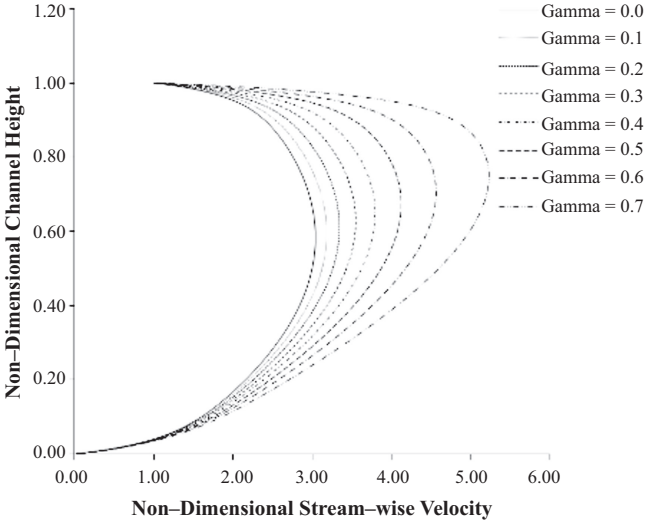

Figure 11.
Numerical variation of stream wise velocity in pressure driven electro-osmotic Couette flow across the channel height with joule heating effect when $\beta = 1000$ and $\alpha = 1$

normal shapes may be clarified in par with the effect of Joule heating. The mean temperature of the dielectric solution is increased by means of Joule heating effect. The increase in temperature affect the dynamic viscosity of the solution and alter the velocity profile in such a way that it varies across the flow direction. This altered velocity profile helps in creating a pumping effect and flow control in microfluidic devices. The inner pressure gradient induced in the flow ensure the conservation of mass and would establish a "suction" effect that results in a fully developed flow.

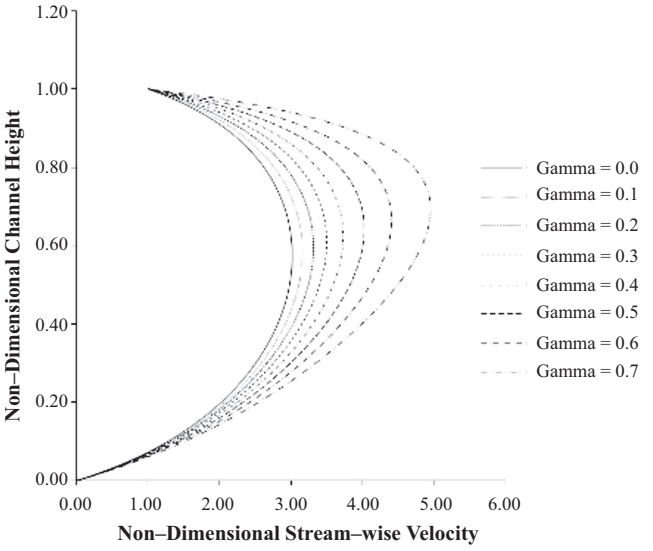

Figure 12.
Numerical variation of stream wise velocity in pressure driven electro-osmotic Couette flow across the channel height with joule heating effect when $\beta = 100$ and $\alpha = 1$

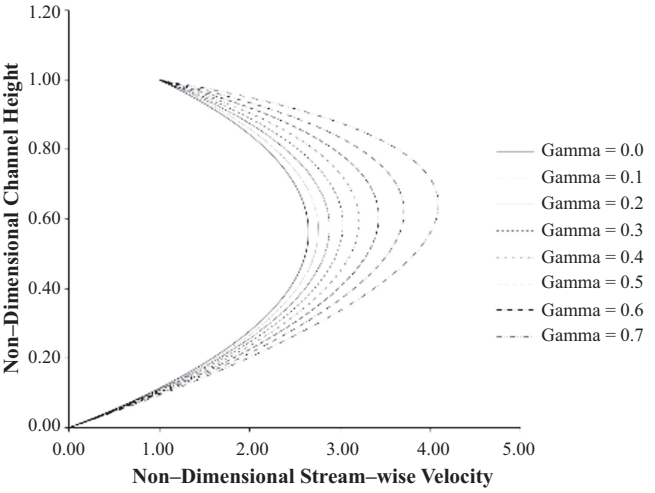

Figure 13.
Numerical variation of stream wise velocity in pressure driven electro-osmotic Couette flow across the channel height with joule heating effect when $\beta = 10$ and $\alpha = 1$

4. Conclusion

The flow control mechanisms in microfluidic/ Nano fluidic devices in the absence of moving components are highly appreciated by the microfluidic scientific community. Numerical investigation on electro-osmotic Couette flow in the presence of Joule heating effect is carried out. The results of the investigation establish that the electro-osmotic Couette flow can be effectively employed as flow control mechanism in microfluidic devices. The effect of Joule heating alter the profile of stream wise velocity from its usual "plug-shaped" nature and assume a convex (parabolic) pattern when the flow is fully developed. The significant

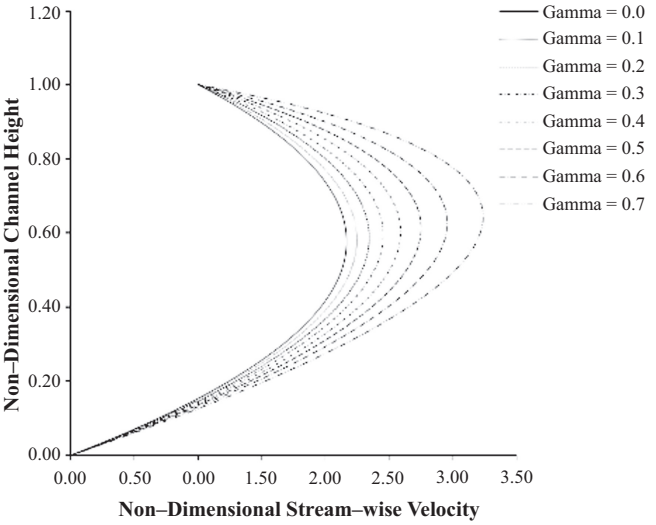

Figure 14.
Numerical variation of stream wise velocity in pressure driven electro-osmotic Couette flow across the channel height with joule heating effect when $\beta = 1$ and $\alpha = 1$

achievement of the present investigation is that it allows a lucid numerical solution to explain the effect of Joule heating on electro-osmotic flow and the associated alterations in stream wise velocity profiles. The developed flow control mechanism may be used for initiating various fluid handling devices like electro-osmotic micro-pumps, micro-valves without any moving components. These long-life microfluidic devices perform without encountering any mechanical failures due to fatigue and much more helpful in biomedical applications, as the damage and denaturation of living cells can be completely eliminated. In short, the current research results may be helpful in efficient and optimum design of numerous microfluidic/nanofluidic devices.

References

Ali, W., Youbing, Z.Æ. and Zhu, Y.Æ.K. (2007), "Couette – Poiseuille flow of a gas in long microchannels", *Microfluid Nanofluid*, Vol. 3, pp. 55-64, doi: 10.1007/s10404-006-0108-5.

Chen, S. and Tian, Z. (2009), "Simulation of microchannel flow using the lattice Boltzmann method", *Physica A*, Vol. 388 No. 23, pp. 4803-4810, doi: 10.1016/j.physa.2009.08.015.

Cummins, E.B., Giffiths, S.K., Nilson, R.H. and Paul, P.H. (2000), "Conditions for similitude between the fluid velocity and electric field in electroosmotic flow", *Analytical Chemistry*, Vol. 72 No. 11, pp. 2526-2532.

Dutta, P. and Beskok, A. (2001a), "Analytical solution of combined electroosmotic/pressure driven flows in two-dimensional straight channels: finite Debye layer effects", *Analytical Chemistry*, Vol. 73 No. 9, pp. 1979-1986, doi: 10.1021/ac001182i.

Dutta, P. and Beskok, A. (2001b), "Analytical solution of time periodic electroosmotic flows : analogies to Stokes' second problem", *Analytical Chemistry*, Vol. 73 No. 21, pp. 5097-5102.

Evenhuis, C.J. (2007), *Thermal Effects and Temperature Profiles in Capillary Electrophoresis*, (Issue January).

Izquierdo, S., Miana, M.J. and Jime, M.A. (2015), "Modelling of Couette flow in microchannels with textured surfaces", *Journal of Engineering Tribology*, Vol. 226, pp. 14-22, doi: 10.1177/1350650111416298.

Kaurangini, M.L. and Jha, B.K. (2011), "Unsteady generalized Couette flow in composite microchannel", *Applied Mathematics and Mechanics*, Vol. 32 No. 1, pp. 23-32, doi: 10.1007/s10483-011-1390-6.

Lo, W.Y. and Chan, K. (1994), "Poisson-Boltzmann calculations of ions in charged capillaries", Vol. 101 April, pp. 1431-1434.

Masliyah, J.H. (2021), "Electrokinetic and colloid transport phenomena 1st edition", *January*, Vol. 2007, pp. 1-4.

Nithiarasu, C.G.T. (2005), "Influences of element size and variable smoothing on inviscid compressible flow solution", *International Journal of Numerical Methods for Heat and Fluid Flow*, Vol. 15 No. 5, pp. 420-428, doi: 10.1108/09615530510593611.

Ohshima, H. (1990), "Electrokinetic flow between two parallel plates with surface charge layers", *Electro-osmosis and Streaming Potential*, Vol. 135 No. 2, pp. 443-448.

Paul, P.H., Garguilo, M.G. and Rakestraw, D.J. (1998). Imaging of pressure- and electrokinetically driven flows through open capillaries. Vol. 70 No. 13, pp. 2459-2467.

Probstein, R.F. (1972), "Desalination: some fluid mechanical problems", *Transactions of the ASME. Series D, Journal of Basic Engineering*, Vol. 94, pp. 286-313.

Probstein, R.F. (2005), *Physicochemical Hydrodynamics: An Introduction*, John Wiley and Sons.

Probstein, R.F. and Hicks, R.E. (1993), "Removal of contaminants from soils by electric fields Ronald", *Science*, Vol. 260 April, pp. 498-503.

Rathore, A.S. (2004), "Joule heating and determination of temperature in capillary electrophoresis and capillary electrochromatography columns", *Journal of Chromatography A*, Vol. 1037, pp. 431-443, doi: 10.1016/j.chroma.2003.12.062.

Reuss., F.F. (1809), "Sur un nouvel effet de l'electricite galvanique", 1809. Memoires de La Societe Imperiale de Naturalistes de Moscou, Vol. 2, pp. 327-337.

Rice, C.L. and Whitehead, R. (1966), "Electrokinetic flow in a narrow cylindrical capillary", *Journal of Physical Chemistry*, Vol. 69 No. 11, pp. 4017-4024.

Rozing, H.H.L. (2018), "High performance capillary electrophoresis", available at: www.agilent.com/chem/CE.

Saleel, C.A., Shaija, A. and Jayaraj, S. (2013), "Computational simulation of fluid flow over a triangular step using immersed boundary method", *International Journal of Computational Methods*, Vol. 10 No. 4, doi: 10.1142/S0219876213500163.

Saleel, C.A., Anjum, I. and Magami, B. (2020), "An immersed boundary method for simulations of flow and mixing in micro-channels with electro kinetic effects", *Progress in Computational Fluid Dynamics, An International Journal*, Vol. 20 No. 2, pp. 93-104, doi: 10.1504/PCFD.2020.106397.

Santiago, J.G. (2001), "Electroosmotic flows in microchannels with finite inertial and pressure forces", *Analytical Chemistry*, Vol. 73 No. 10, pp. 2353-2365, doi: 10.1021/ac0101398.

Schasfoort, R.B.M., Schlautmann, S. and Jan Hendrikse, A.V.B. (1999), "Field-effect flow control for microfabricated fluidic networks R", *Science*, Vol. 286 October, pp. 942-945.

Corresponding author
C. Ahamed Saleel can be contacted at: ahamedsaleel@gmail.com